

Ground motion observations and simulation for local earthquakes in the Campi Flegrei volcanic area

Danilo Galluzzo¹ · Francesca Bianco¹ ·
Mario La Rocca¹ · Gaetano Zonno²

Received: 15 December 2014 / Accepted: 29 April 2015 / Published online: 10 May 2015
© Springer Science+Business Media Dordrecht 2015

Abstract Ground motion produced by low magnitude earthquakes can be used to predict peak values in high seismic risk areas where large earthquakes data are not available. In the present work 20 local earthquakes ($M_D \in [-0.3, 2.2]$) occurred in the Campi Flegrei caldera during the last decade were analyzed. We followed this strategy: empirical relations were used to calibrate synthetic modeling, accounting for the source features and wave propagation effects. Once the source and path parameters of ground motion simulation were obtained from the reference data set, we extrapolated scenarios for stronger earthquakes for which real data are not available. The procedure is structured in two steps: (1) evaluation of ground motion prediction equation for Campi Flegrei area and assessment of input parameters for the source, path and site effects in order to use the finite fault stochastic approach (EXSIM code); (2) simulation of two moderate-to-large earthquake scenarios for which only historical data or partial information are available ($M_w 4.2$ and $M_w 5.4$). The results show that the investigated area is characterized by high attenuation of peak amplitude and not negligible site effects. The stochastic approach has revealed a good tool to calibrate source, path and site parameters on small earthquakes and to generate large earthquake scenario. The investigated magnitude range represents a lower limit to apply the stochastic method as a calibration tool, due to the small size of involved faults (fault length around 200/300 m).

✉ Danilo Galluzzo
danilo.galluzzo@ingv.it

Francesca Bianco
francesca.bianco@ingv.it

Mario La Rocca
mario.larocca@ingv.it

Gaetano Zonno
gaetano.zonno@ingv.it

¹ Istituto Nazionale di Geofisica e Vulcanologia, Osservatorio Vesuviano, Via Diocleziano, 328, 80124 Naples, Italy

² Istituto Nazionale di Geofisica e Vulcanologia, Milan, Italy

Keywords Stochastic simulation · Peak velocity · Campi Flegrei

1 Introduction

Ground motion simulation in volcanic areas is a difficult task due to the complexity of seismic source, heterogeneity of the propagation medium and surface geomorphological features. In regions where large earthquake data are not available we can use the ground motion produced by small size earthquakes to simulate the ground shaking likely associated with larger events. This is the case of Campi Flegrei caldera, an active volcanic area located in southern Italy, west of Naples. Two caldera collapses [Campanian Ignimbrite, 39 ka; Neapolitan Yellow Tuff (NYT), 15 ka] have contributed to define the present structural setting of Campi Flegrei (Selva et al. 2011). In the past 15 ka, volcanic activity has been concentrated within NYT caldera; the last eruption occurred in 1538 (Mt. Nuovo eruption) after a long period (LP) of quiescence. During the last century the two major unrest episodes occurred in 1969–1972 and 1982–1984. During the latter episode, when a ground uplift of 2 m occurred, more than 16,000 shallow earthquakes were recorded, the most of which were located in Pozzuoli-Solfatara area (central sector of the volcanic area). The maximum duration magnitude was 4.2 (Aster et al. 1992), while the maximum macroseismic intensity was VI/VII degree (Branno et al. 1984). Minor swarms of volcano tectonic (VT) seismicity occurred in 2000 (maximum $M_D = 2.2$, Saccorotti et al. 2001) and 2006 (maximum $M_D = 1.4$, Saccorotti et al. 2007), while a large swarm of LP events was recorded in 2006. Focal mechanisms evaluated for 2006 VT events show a predominance of normal faults, with stress drop values between 1 and 10 bar (Saccorotti et al. 2007). Several studies were performed to investigate source features (e.g. Del Pezzo et al. 1987), propagation characteristics (e.g. Petrosino et al. 2008) and site effects (e.g. Tramelli et al. 2010). The present structural setting of the caldera is dominated by faults, fractures and morpho-structural elements related with the volcanic history of the area. Fault main trends are NE–SW and NW–SE, while only a few are around N–S and E–W fault alignments are observed. A detailed description of historical volcanism and structural setting can be found in the work of Selva et al. (2011).

Some efforts have been done to assess ground motion parameters peak ground velocity (PGV), peak ground acceleration (PGA) and peak spectral acceleration (PSA) based on empirical observations and stochastic simulation of the source (e.g. De Natale et al. 1988; Galluzzo et al. 2004; Douglas et al. 2013), or probabilistic approach (e.g. Convertito and Zollo 2011). The present study is part of a European project (UPStrat_MAFa: Urban disaster Prevention Strategies using MACroseismic Fields and FAUlt Sources) in which several volcanic areas were studied. In the present paper we adopted a simulation procedure to calculate ground motion scenarios associated with large earthquakes that can potentially strike the area of Campi Flegrei. Before applying a stochastic procedure to simulate strong ground motion, all parameters and physical quantities must be tuned by comparing simulated and observed PGV and response spectra. To achieve this goal we adopted the finite fault stochastic method by Motazedian and Atkinson (2005). First we evaluated ground motion prediction equation (GMPE) for small local earthquakes of Campi Flegrei and later we compared observed and simulated ground motion to assess a set of input parameters representative of the true ground motion. The last step consisted in the evaluation of moderate-to-large earthquake scenarios based on historical parametric data.

The data set used in the present study is composed of twenty well located earthquakes ($M_D \in [-0.3, 2.2]$, maximum hypocentral distance $R = 12$ km) recorded in the Campi Flegrei caldera in the period 2000–2012 (Tables 1, 2; Fig. 1). The five earthquakes with the best signal-to-noise ratio recorded by the largest number of stations were used to compare observed and simulated ground motion in order to calibrate input parameters for simulations, as explained in the next section. Figure 2 shows the seismograms of horizontal components for one of selected earthquakes recorded at seven stations (earthquake 20120907 0734, M_w 2.2).

2 Method of analysis

We started our analysis by computing GMPE on twenty local earthquakes. The general formulation of GMPE equation is:

$$F(Y) = a f_1(M) + b f_2(R) + c + \sigma, \quad (1)$$

where $F(Y)$ is a function of ground acceleration or velocity, $f_1(M)$ and $f_2(R)$ are functions of magnitude M and distance R respectively. Taking into account the small ranges of magnitudes, focal depths and epicentral distances, we assumed $F(Y)$ equal to $\log_{10}(\text{PGV})$, $f_1(M)$ as a linear function of moment magnitude and $f_2(R)$ equal to $\log(R)$. Consequently GMPE was evaluated by fitting the PGV values with a non linear model given by the equation:

Table 1 Hypocenters and magnitude of earthquakes considered in this work

Date (yymmdd hhmm)	Lat (°)	Lon (°)	Depth (km)	M_D
20120907 0825	40.836	14.111	3.0	1.7
20120907 0734	40.836	14.111	3.0	1.8
20110908 0256	40.823	15.146	1.9	1.2
20110519 0039	40.842	14.177	3.1	1.5
20110418 0143	40.825	14.136	1.9	-0.3
20110410 1210	40.879	14.111	4.4	1.4
20110207 0703	40.845	14.135	1.7	1.1
20110205 1626	40.823	14.159	3.8	-0.3
20101106 1621	40.870	14.086	6.1	0.8
20100707 1316	40.821	14.133	1.4	-0.1
20100330 1638	40.835	14.149	2.1	0.2
20100129 1734	40.855	14.150	3.1	1.1
20080219 1248	40.849	14.182	3.9	1.6
20061221 2225	40.843	14.146	1.6	1.4
20061221 2242	40.842	14.145	1.2	1.1
20061220 2353	40.826	14.153	2.2	1.1
20061028 1757	40.825	14.153	1.7	0.2
20060408 0709	40.829	14.147	2.3	0.9
20060206 0932	40.829	14.169	3.1	0.4
20000822 1558	40.828	14.145	2.7	2.2

Table 2 Coordinates of the seismic stations used in this work

Station	Lat (°)	Lon (°)
ACL2	40.8836	14.0706
AMS2	40.8264	14.1604
ASB2	40.8435	14.1458
BGNG	40.8189	14.1454
BULG	40.8312	14.1627
CELG	40.8320	14.1231
MSGG	40.8424	14.1824
OMN2	40.8329	14.0903
OVDG	40.8197	14.1828
PESG	40.8323	14.1532
RENG	40.8263	14.1507
SETG	40.8304	14.1358
SLF	40.8291	14.1397
AFB	40.8426	14.2348
SSV	40.8795	14.0707
TAGG	40.8293	14.1736
CUBB	40.8479	14.0543

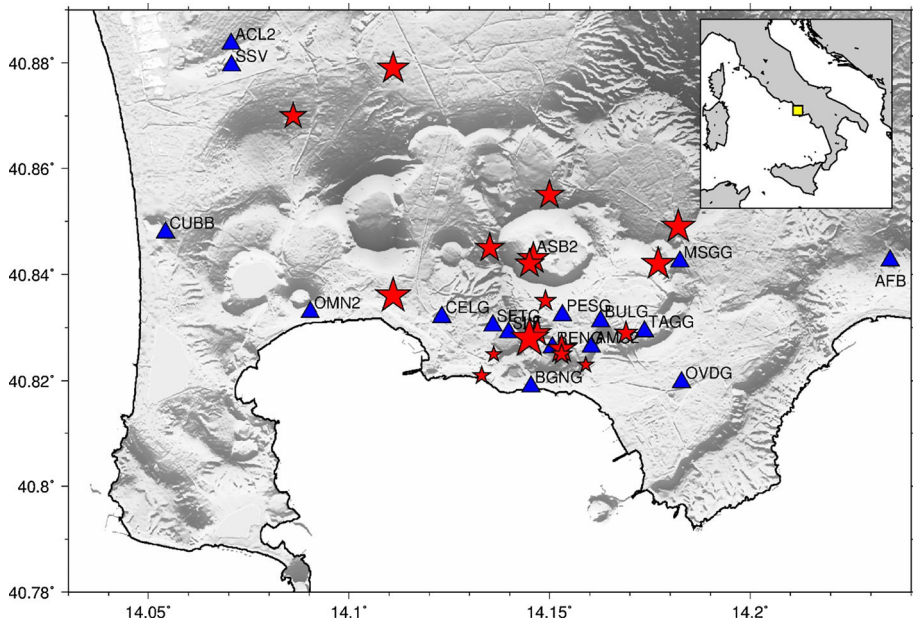


Fig. 1 Epicenters of analyzed earthquakes (*red stars*) and seismic stations (*blue triangles*) in the Campi Flegrei area. The size of *star symbol* is proportional to the earthquake magnitude. The *yellow square* in the *inset map* of Italy shows the position of Campi Flegrei

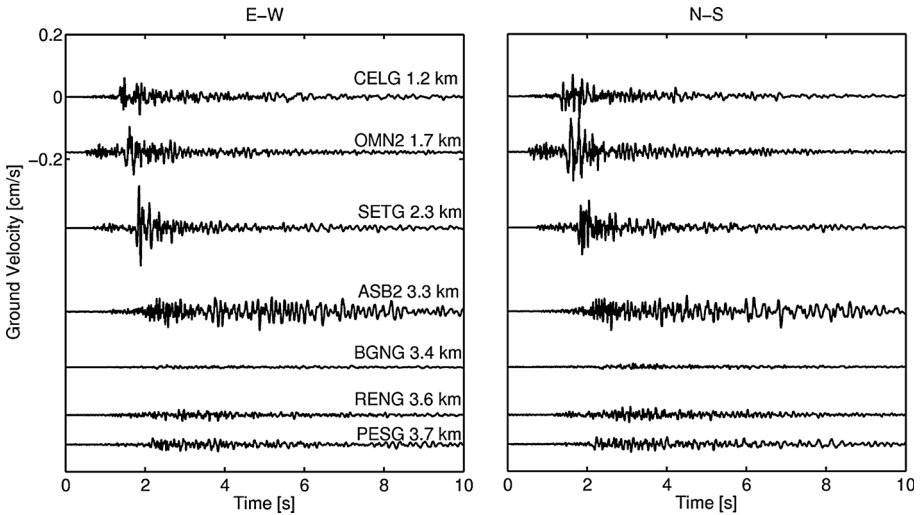


Fig. 2 Horizontal components of ground velocity (E–W on the left, N–S on the right) produced by the earthquake 20120907 0734, M_w 2.2, recorded at six seismic stations. The waveforms are plotted with epicentral distance (1–4 km) increasing from top to bottom, as indicated inside the figure

$$\log_{10}(\text{PGV}) = a + b M_w + c \log_{10}R + \sigma_{\text{Log}Y}, \tag{2}$$

where PGV (cm/s) indicates the PGV on horizontal (or vertical) components of motion, M_w is the moment magnitude and R (km) is the hypocentral distance. PGV on horizontal components was set by considering the maximum value between the N–S and E–W components.

Following Havskov and Ottemoller (2010), preliminary M_w was evaluated from the seismic moment M_0 (Hanks and Kanamori 1979), computing the low frequency spectral amplitude averaged on all available stations. The seismic moment M_0 was calculated by considering the relationship (Lay and Wallace 1995):

$$M_0 = \frac{4\pi\rho v_s^3 R \Omega_0}{F Y_{0,\phi}} \tag{3}$$

where ρ is the density of the medium, v_s is the shear wave velocity at source, R the hypocentral distance, Ω_0 the low-frequency level of the source displacement spectrum, F the free surface operator ($F = 2$) and $Y_{0,\phi}$ the radiation pattern term. Attenuation parameters, density, and shear wave velocity model were taken from the papers of Petrosino et al. (2008), Aster et al. (1992) and Aster and Meyer (1988) respectively. For seismic moment evaluation, geometrical spreading was set to $1/R$ and radiation pattern term was set to the average value of 0.55.

The attenuation terms were deconvolved from the displacement spectra (evaluated on 1 s window starting 0.2 s before S wave arrival and averaged on the horizontal component of motion), before evaluating low frequency spectral level of seismic source. Low frequency spectral amplitude was evaluated in the frequency range between 2 and 6 Hz. M_w was calculated from M_0 at each site and averaged over all the available stations. The average can reduce the effect of local amplification at a single site. By considering the previous procedure we obtain an error of 0.3–0.4 on the estimate of M_w .

After the estimation of GMPE we have calibrated input ground motion parameters for stochastic simulation (magnitude, fault size and subdivision, stress drop, and attenuation features). Hence, the second step was to select five local earthquakes characterized by the largest number of recording sites. We have used the finite fault stochastic approach by Motazedian and Atkinson (2005) coded in the software EXSIM. The basic principle of finite fault stochastic approach is based on the assumption that, considered a target fault subdivided in subfaults, the ground motion acceleration (the same occurs for velocity) $a(t)$ is obtained by summing with a proper delay time all the contributions from each subfaults as:

$$a(t) = \sum_{i=1}^{nl} \sum_{j=1}^{nw} a_{ij}(t + \Delta t_{ij}), \tag{4}$$

where nl and nw are the number of subfaults along the fault length and width, and Δt_{ij} is the radiation delay time from the ij -th subfault to the observation point. Each time series $a_{ij}(t)$

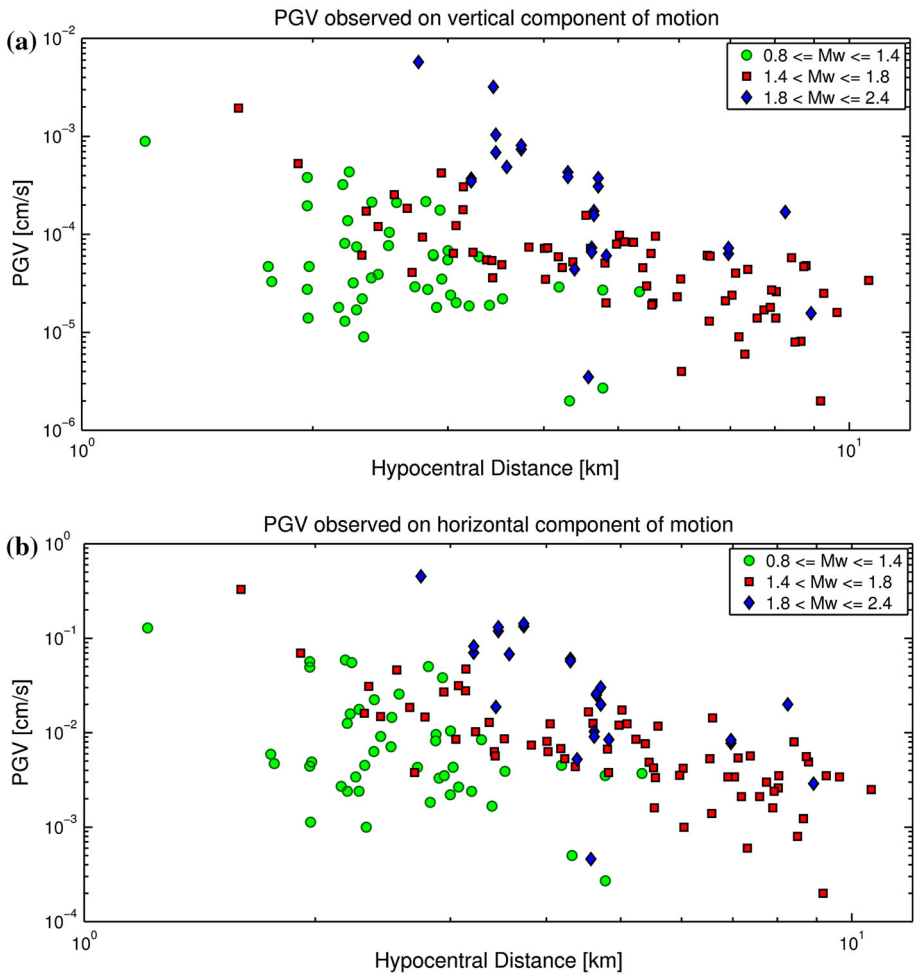


Fig. 3 Peak ground velocities **a** vertical PGV, **b** horizontal PGV observed for 20 local earthquakes occurred in Campi Flegrei area between 2000 and 2012

is stochastically generated by assuming that the corresponding spectrum $A_{ij}(f)$ can be modeled by an ω -squared shape (Boore 1983) as:

$$A_{ij}(f) = \frac{1}{R_{ij}} \frac{CM_{0ij}(2\pi\pi)^2}{1 + (f_{0ij})^2} \exp(-\pi f\kappa) \cdot \exp\left(\frac{-\pi f R_{ij}}{Q\beta}\right), \tag{5}$$

where M_{0ij} , f_{0ij} and R_{ij} are the ij -th subfault seismic moment, corner frequency and distance from the observation point, respectively. The constant C includes radiation pattern, free surface amplification, horizontal components partition factor, density and shear wave velocity at the source. The term $\exp(-\pi f\kappa)$ is relative to high frequency fall off decay (Anderson and Hough 1984) and can be alternatively modeled by f_{max} filter. The term $1/R_{ij}$ and the quality factor $Q(f)$ are related to geometrical spreading and elastic attenuation, respectively. The seismic moment M_{0ij} associated to each subfault is obtained by dividing the seismic moment M_0 associated to the entire fault by the number N of total subfaults, being $N = nl \times nw$. In case the slip on the entire fault is not uniform, M_{0ij} is obtained by considering a specific weight associated to the relative slip of the ij -th subfault. In the present study, the simulated PGV and response spectra (5 % of damping) were obtained by averaging among 50 simulations. To check the validity of the simulation parameters retrieved from other studies we compared PGV and spectral response spectra of observed and simulated ground motion through a quantitative fit method as explained in the next section. Finally, with the well-tuned set of parameters, we have simulated the ground motion produced by strong earthquakes occurred in the past centuries, known from historical seismicity and parametric catalog.

3 Results

Before the evaluation of empirical relationship for PGV, the seismic moment M_0 (and hence M_w) was calculated for the 20 selected earthquakes. The obtained range of magnitude is $M_w \in [0.8, 2.4]$ (corresponding to $M_D \in [-0.3, 2.2]$). PGV was measured on the vertical and horizontal components of motion for all selected earthquakes. The peak velocity versus hypocentral distance is shown in Fig. 3 for different ranges of magnitude. By fitting the data shown in Fig. 3 with Eq. (2) we obtained the corresponding parameters for GMPE relationship (for vertical and horizontal components of motion), as shown in Table 3. This GMPE relationship is valid in the overall range of magnitude $M_w \in [0.8, 2.4]$. For such a low magnitude range, that has no direct application for seismic hazard, very few GMPEs are found in literature. In Fig. 4 we compare the GMPE found in this work with GMPEs evaluated for the volcanic area of Etna (Langer et al. 2015) and Irpinia (Bobbio

Table 3 Regression coefficients and associated standard errors for PGV (horizontal and vertical) relationship in Eq. (1)

Y (cm s ⁻¹)	A	b	c	< σ_{LogY} >
PGVh	-2.45 ± 0.02	1.19 ± 0.01	-2.54 ± 0.04	0.1
PGVz	-2.65 ± 0.02	1.22 ± 0.01	-2.52 ± 0.04	0.1

Uncertainties (σ) of coefficients are referred to a confidence interval of 95 % and must be considered an average uncertainties over the whole range of magnitude

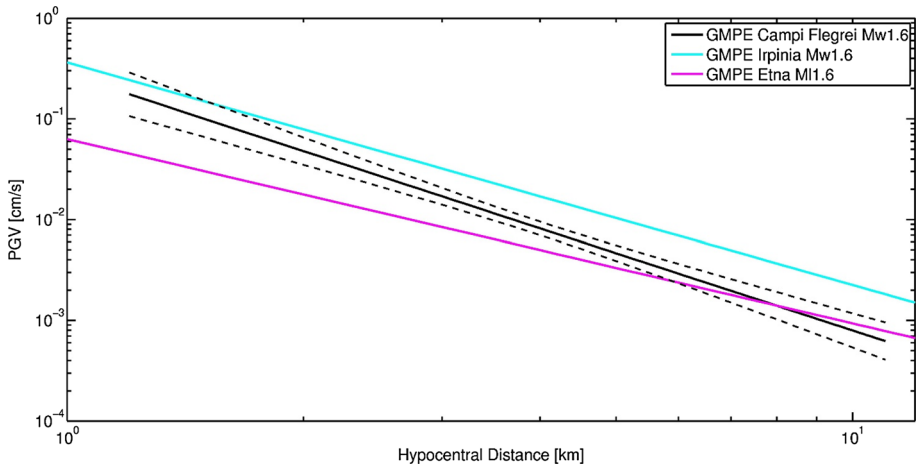


Fig. 4 Campi Flegrei GMPE for $M_w 1.6 \pm \sigma$ (black continuous line and dotted lines) compared with Irpinia GMPE $M_L 1.6$ (cyan continuous line, Bobbio et al. 2009) and Etna GMPE $M_L 1.6$ shallow earthquakes (magenta continuous line)

Table 4 Input parameters for the generation of synthetic ground motion in Campi Flegrei area using the program EXSIM

Parameters	Value	References
Stress drop $\Delta\sigma$ (bar)	1–20 bar	Del Pezzo et al. (1987)
Crustal S-wave velocity	$V_s = V_s(Z)$	Aster and Meyer (1988), currently used at INGV-Napoli
Crustal density	2.2 g/cm ³	Aster et al. (1992)
Kappa	0.015	De Natale et al. (1988)
Geometric spreading	$R^{-0.8}$	Calibrated starting from assumed $R^{-1.0}$ (Del Pezzo et al. 1987; Tramelli et al. 2010)
Q(f)	$25 f^{0.4}$	Calibrated starting from evaluated $Q(f) = 21 f^{0.6}$ (Petrosino et al. 2008)
Distance dependent duration	$T_0 + 0.9R$	Galluzzo et al. (2008)
Windowing function	Saragoni–Hart	–
Rupture propagation	0.8 V_s	–
Slip distribution	Random	–
Pulsing area percentage	50 %	–

et al. 2009), a tectonic active area about 90 km East of Campi Flegrei. Although we compare M_w with M_L scale (in the case of $M_w 1.6$), it is noteworthy that the attenuation of peak velocity for Campi Flegrei (black line) is stronger than that of the other two areas (magenta and cyan lines).

The evaluated GMPE was used to calibrate the set of parameters for the stochastic simulation. The calibrated set of parameters was fixed by comparing simulated and observed ground motion. The synthetic seismograms closest to the observed ones were set by a trial and error procedure performing a grid search of the best solution on various input parameters retrieved from other studies. The best solution was chosen on the base of GOF test (Good Of Fitness based on normalized root mean square error) between observed and

simulated PGV. The simulations were performed for shear waves, therefore the comparison was done with the horizontal components of ground motion. The set of input parameters for the finite fault stochastic procedure is shown in Table 4 with the respective references. The comparison between observed and simulated ground motion was carried out on 5 selected earthquakes. In Fig. 5 we show the cases of three earthquakes (20120907 0734 M_w 2.2, 20111004 1211 M_w 1.8, 20110519 0039 M_w 1.5), in terms of PGV trend for horizontal components of motion. The source parameters used for the simulations shown in Fig. 5 are resumed in Table 4. The hypocenters were assumed to be located at the fault center and random slip distribution was set. Fault size and stress drop were set on the base of source scaling analysis (Del Pezzo et al. 1987), while focal mechanisms were evaluated through the FOCMEC code (Snoko 2003). As an example, in Fig. 5d we show the GOF test for different values of stress drop: the best fit is obtained for $\Delta\sigma = 5$ bar. The simulated values of PGV reproduce the GMPE trend, even though sometimes the observed values are much higher than predicted ones. The high variability of the peak amplitude and the shape of waveforms is typical of Campi Flegrei area. This is clearly seen in Fig. 2, where the signals of the earthquake 20120907 0734 (Table 5) are shown with epicentral distance increasing from top to bottom. This observation can be explained by the local site effects in the area; Tramelli et al. (2010) showed that for some sites there are relative amplifications of a factor 3 or 4 in the frequency band 1–20 Hz. The comparison between observed and simulated response spectra for the 20120907 0734 earthquake is shown in Fig. 6 at four sites. The simulated response spectra are quite similar to those observed on the horizontal component of motion.

Once the calibrated parameters were tuned, we performed two simulations for the moderate-to-large earthquake scenarios. To define the possible moderate-to-large earthquake that could occur in the area, we considered the following results from literature: the largest magnitude earthquake occurred during the 1982–1984 bradyseismic episode ($M = 4.2$, Aster et al. 1992); the maximum expected magnitude $M = 4.3$ (Galluzzo et al. 2004), and the largest earthquake from the historical parametric catalog CPTI11 ($M = 5.4$ occurred in 1582, Rovida et al. 2011). For the sake of simplicity hereafter we refer to the previous magnitude scales as moment magnitude M_w . We have performed two simulations, one for $M_w = 4.2$ and another for $M_w = 5.4$. Chosen an arbitrary epicenter, we have generated PGV along radial distance by averaging over all directions. By using the calibrated parameters shown in Table 4, the stochastic simulation for the two earthquake scenarios have been performed. For M_w 4.2 we have adopted the source depth at 2.7 km b.s.l., stress drop values equal to 5, 10, 20 and 30 bar and fault size of 2 km \times 1 km. In the case of M_w 5.4 we set arbitrarily the depth at 4 km b.s.l., stress drop values equal to the M_w 4.2 case and fault size of 6 km \times 5 km, considering the results of Konstantinou (Konstantinou 2014) obtained for the Mediterranean region. The results are shown in Figs. 7 and 8 for M_w 4.2 and M_w 5.4 respectively. Superimposed to PGV trend in the case of M_w 4.2, we plotted, in Fig. 7, the GMPEs from Langer et al. (2015) obtained in the volcanic area of Mt Etna for superficial events in the magnitude range M_L [3,4.8].

4 Discussion and conclusions

The observations about low magnitude local earthquakes (M_D [-0.3, 2.2]; M_w [0.8, 2.4]) occurred in Campi Flegrei area show high variability among the different sites in terms of PGV, waveform shape and spectral content. The use of a stochastic simulation procedure

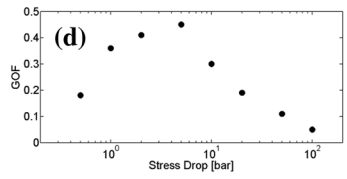
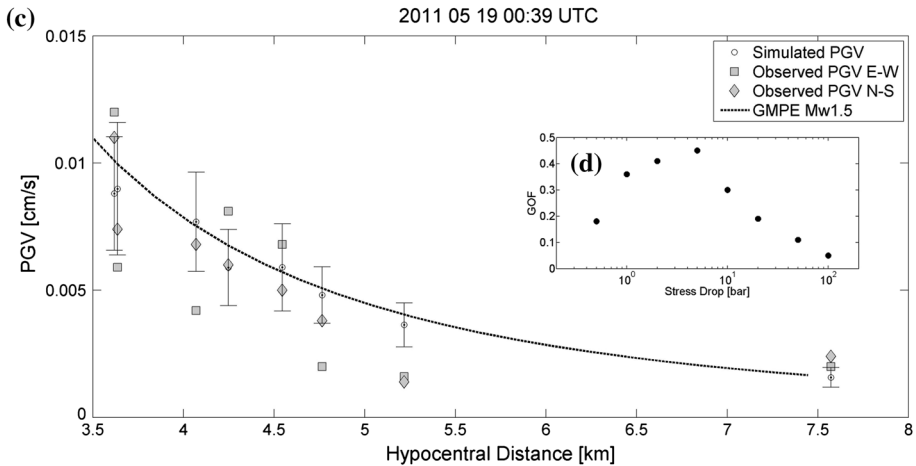
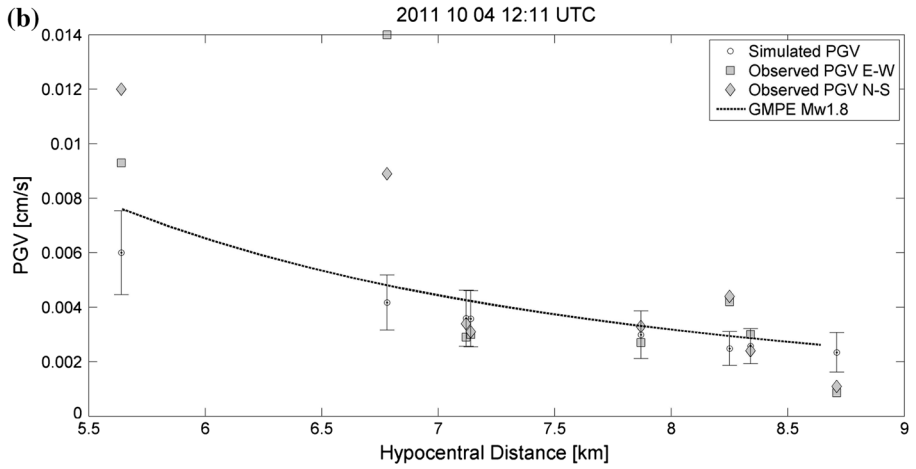
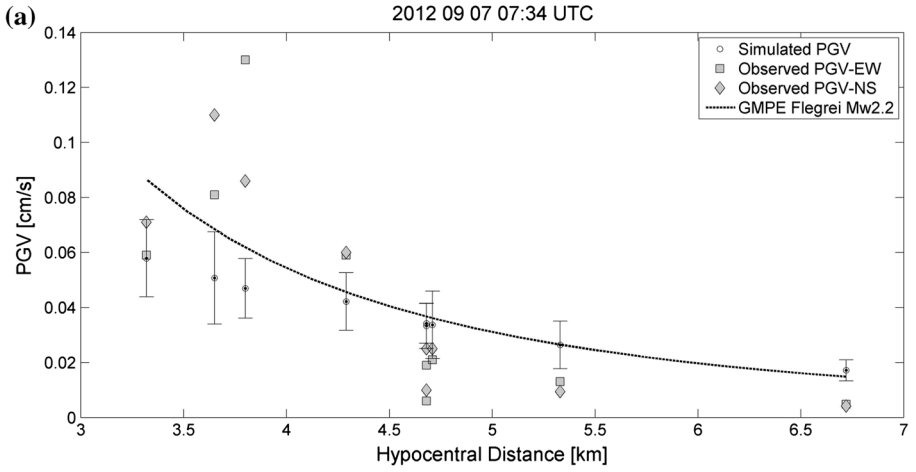


Fig. 5 Comparison between PGV values observed on horizontal components (*gray full squares and diamonds*), GMPE evaluated for Campi Flegrei (*dotted line*) and simulated PGV (*circles with error bars*). Results are shown for three specific earthquakes of magnitude M_w 2.2 (**a**), M_w 1.8 (**b**) and M_w 1.5 (**c**). **d** M_w 1.5 GOF test obtained for different values of stress drop

Table 5 Source parameters, seismic stations and epicentral distance of local earthquakes used for the calibration procedure

Date (UTC)	Lat (°)	Lon (°)	Depth (km)	M_w	$\Delta\sigma$	Strike (°)	Dip (°)	L × W (m ²)
20120907 07:34	40.836	14.111	3.0	2.2	5	10	65	300 × 300
Stations	CELG, OMN2, SETG, ASB2, BGNG, RENG, PESG, ACL2							
Epi. distance range (km)	1.2–6.3							
20111004 12:11	40.879	14.111	4.4	1.8	5	320	42	200 × 200
Stations	ACL2, OMN2, ASB2, CELG, RENG, BGNG							
Epi. distance range (km)	3.4–7.3							
20110519 00:39	40.842	14.177	3.1	1.5	5	96	85	200 × 200
Stations	BULG, PESG, OVDG, ASB2, RENG, SETG, BGNG, ARF3, OMN2							
Epi. distance range (km)	1.7–7.3							
20080219 12:48	40.849	14.182	3.9	1.8	5	275	50	200 × 200
Stations	TAGG, ASB2, OVDG, AMS2, BGNG, OMN2							
Epi. distance range (km)	2.3–7.9							
20061221 22:25	40.843	14.146	1.6	1.5	5	346	66	200 × 200
Stations	ASB2, AMS2, BGNG, TAGG, OVDG, OMN2, CUBB							
Epi. distance range (km)	0–8.5							

The calibration for the first three earthquakes is shown in Figs. 5 and 6

allowed us to calibrate source (fault size, stress drop) and propagation (attenuation Q) parameters by comparing observations and simulated waveforms, which are averaged over the selected set of earthquakes and over the area of study. This analysis has been performed for the five well recorded earthquakes and has shown the following features: fault size of 200/300 m, stress drop of about 5 bar, and Q attenuation factor ($Q_s = 25 \cdot f^{0.4}$) very close to values described in literature. Both GMPE trend and Q_s have revealed a considerable attenuation which characterizes the investigated area, as confirmed by the comparison with other volcanic and tectonic environments. It is not simple to quantify the influence of site effect on simulated results. Simulated PGV and response spectra were obtained by averaging the results over 50 simulations but in some cases the observed PGV are quite larger than the simulated ones. The difference between observed and simulated trend (most of them 3–4 times greater than the simulated PGV) indicates the presence of site effects in the area.

The tuned parameters and simulation method allowed us to simulate ground motion scenario for large earthquakes that could strike the area. In the specific case we have selected, on the base of published works and catalogs, the M_w 4.2 and M_w 5.4 earthquakes to perform ground motion simulation. In synthesis, for Campi Flegrei the main results of this study are:

- Large variability of peak velocity in the area due to local site effects;

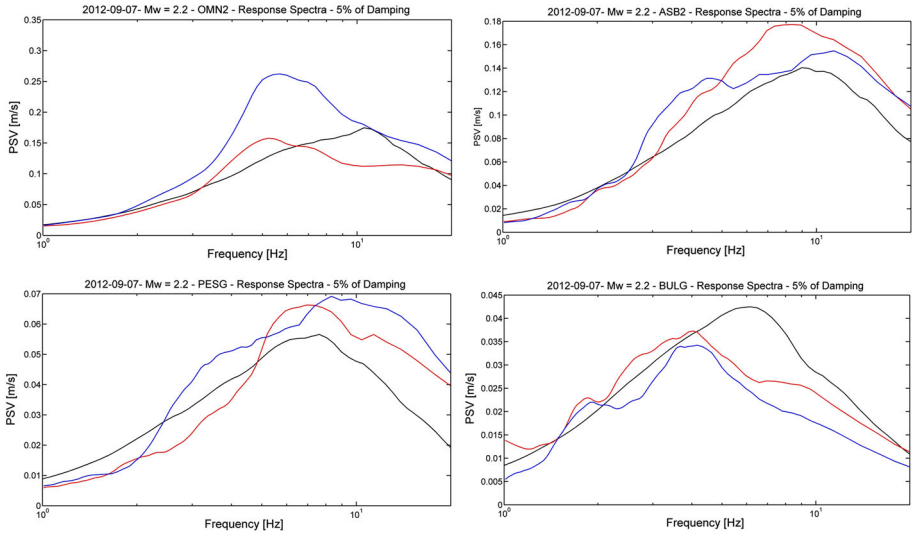


Fig. 6 Observed (red and blue lines for E–W and N–S components respectively) and simulated response spectra (black line; 5 % of damping averaged on 50 simulations) for the earthquake 20120907 07:34, Mw2.2, at four stations

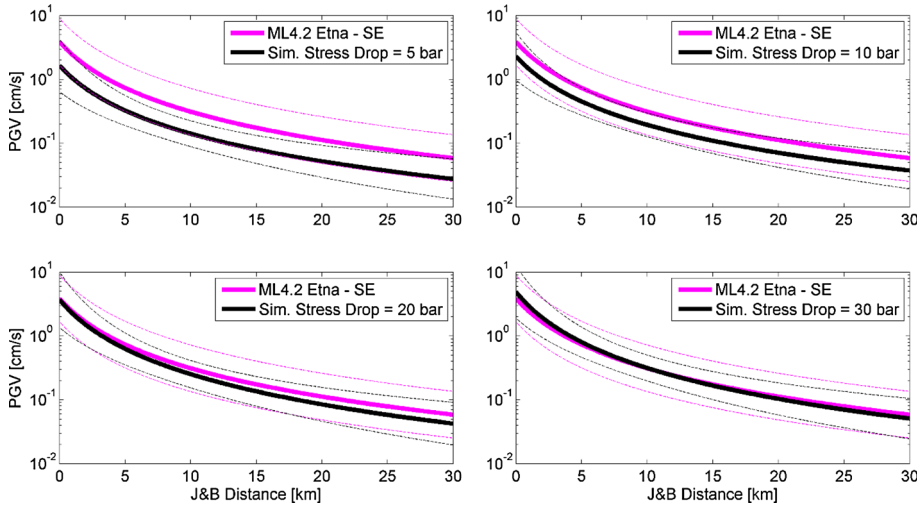


Fig. 7 Comparison of simulated ground motion PGV for M_w 4.2 (black line) with hypocenter at 2.7 km depth for different values of stress drop (5, 10, 20 and 30 bar), and M_L 4.2 GMPE for Mt Etna Superficial Events (from Langer et al. 2015, magenta line)

- Strong attenuation that affects the amplitude trend far from epicenter;
- The simulated PGV takes a maximum value of 4 cm/s for M_w 4.2 (depth = 2.7 km, $\Delta\sigma = 30$ bar), and 7 cm/s for M_w 5.4 (depth = 4.0 km, $\Delta\sigma = 30$ bar) simulated amplitude;

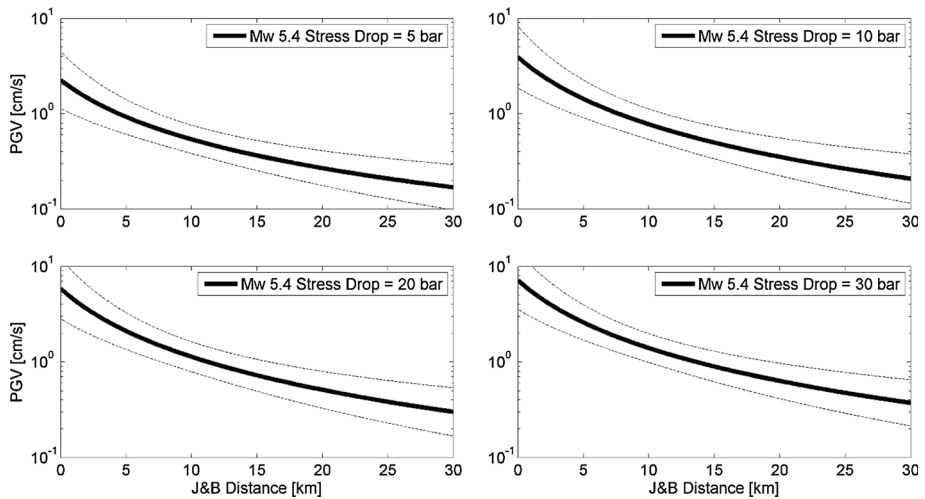


Fig. 8 Simulated ground motion PGV for Mw5.4 (*black line*) with hypocenter at 4.0 km depth for different values of stress drop

- The simulated PGV for $M_w 4.2$ shows similar values to PGV obtained for Mt Etna ($M_L = 4.2$) for a stress drop of 30 bar. Taking into account the difference between M_L and M_w scale ($M_w - M_L = 0.3$ as deduced from Azzaro et al. 2011) we are confident that the two curves show similar results in a stress drop range of 10–30 bar. Imcs intensities calculated from PGV (Faenza and Michelini 2010) are equal to 6–7 (in the range 10–30 bar) and are similar to the values found by Branno et al. (1984);
- The simulated PGV for $M_w 5.4$ gives Imcs value equal to 7, and only in some cases, for stress drop of 30 bar, equal to 8. These values are in agreement with the value (7–8) reported by Rovida et al. (2011).

The stochastic approach has revealed an useful tool to investigate source, path and site effect features in heterogeneous environment as volcanic areas, characterized by low magnitude seismicity. More efforts should be addressed to understand the influence of site amplification on the GMPE evaluation and on stochastic simulations. However, the stochastic finite fault approach coded in EXSIM has been an useful tool to simulate strong ground motion scenario although, for low magnitude local seismicity, fault size of hundreds of meters represents a lower limit for the application of the method which has been implemented for larger earthquakes.

Acknowledgments This study was co-financed by the EU-Civil Protection Financial Instrument (Urban disaster Prevention Strategies using MACroseismic Fields and FAult Sources-UPStrat-MAFA, Grant Agreement N. 23031/2011/613486/SUB/A5).

References

- Anderson J, Hough S (1984) A model for the shape of Fourier amplitude spectrum of acceleration at high frequencies. *Bull Seismol Soc Am* 74:1969–1993
- Aster RC, Meyer RP (1988) Three-dimensional velocity structure and hypocenter distribution in the Campi Flegrei caldera, Italy. *Tectonophysics* 149(3–4):195–218. <http://www.sciencedirect.com/science/journal/00401951/149/3>

- Aster RC, Meyer RP, De Natale G, Zollo A, Martini M, Del Pezzo E, Scarpa R, Iannaccone G (1992) Seismic investigation of the Campi Flegrei Caldera, in “Volcanic Seismology”. Proc. Volcanol. Ser. III, Springer Verlag, New York
- Azzaro R, D’Amico S, Tuvè T (2011) Estimating the magnitude of historical earthquakes from macroseismic intensity data: new relationships for the volcanic region of Mount Etna (Italy). *Seismol Res Lett* 82(4):533–544
- Bobbio A, Vassallo M, Festa G (2009) A local magnitude scale for southern Italy. *Bull Seismol Soc Am* 95:592–604
- Boore DM (1983) Stochastic simulation of high-frequency ground motions based on seismological models of the radiated spectra. *Bull Seismol Soc Am*. 73:1865–1894
- Branno A, Esposito E, Luongo G, Marturano A, Porfido S, Rinaldis V (1984) The October 4th, 1983 magnitude 4 earthquake in Phlegraean fields: macroseismic survey. *Bull Volcanol* 47–2:1984
- Convertito V, Zollo A (2011) Assessment of pre- and syn-crisis seismic hazard at Mt. Vesuvius and Campi Flegrei volcanoes, Campania region southern Italy. *Bull Volcanol*. doi:10.1007/s00445-011-0455-2
- De Natale G, Faccioli E, Zollo A (1988) Scaling of peak ground motions from digital recordings of small earthquakes at Campi Flegrei, southern Italy. *Pure appl Geophys* 126(1):37–53
- Del Pezzo E, De Natale G, Martini M, Zollo A (1987) Source parameters of microearthquakes at Phlegraean fields (Southern Italy) volcanic area. *Phys Earth Planet Inter* 47:25–42
- Douglas J, Edwards B, Convertito V, Sharma N, Tramelli A, Kraaijpoel D, Cabrera BM, Maercklin N, Troise C (2013) Predicting ground motion from induced earthquakes in geothermal areas. *Bull Seismol Soc Am* 103(3):1875–1897
- Faenza L, Michelini A (2010) Regression analysis of MCS intensity and ground motion parameters in Italy and its application in ShakeMap. *Geophys J Int* 180:11138–11152
- Galluzzo D, Del Pezzo E, La Rocca M, Petrosino S (2004) Peak ground acceleration produced by local earthquakes in volcanic areas of Campi Flegrei and Mt. Vesuvius. *Ann Geophys* 47(4):1377–1389
- Galluzzo D, Del Pezzo E, Zonno G (2008) Stochastic finite-fault ground-motion simulation in a wave-field diffusion regime: case study of the Mt. Vesuvius Volcanic area. *Bull Seismol Soc Am* 98(3):1272–1288. doi:10.1785/0120070183
- Hanks M, Kanamori H (1979) A moment magnitude scale. *J Geophys Res* 84:2348–2350
- Havskov J, Ottemoller L (2010) Routine data processing in earthquake seismology: with sample data, exercises and software. Springer, Netherlands
- Konstantinou KI (2014) Moment magnitude–rupture area scaling and stress-drop variations for earthquakes in the Mediterranean region. *Bull Seismol Soc Am* 104(5):2378–2386
- Langer H, Tusa G, Scarfi L, Azzaro R (2015) Ground motion scenarios on Mt Etna from empirical relations and synthetic simulations. *Bull Earthquake Eng (UPStrat MAFA Special Issue)*
- Lay T, Wallace TC (1995) Modern global seismology. Academic Press, London
- Motazedian D, Atkinson GA (2005) Stochastic finite-fault modeling based on a dynamic corner frequency. *Bull Seimol Soc Am* 95(3):995–1010
- Petrosino S, De Siena L, Del Pezzo E (2008) Recalibration of the magnitude scales at Campi Flegrei, Italy, on the basis of measured path and site and transfer functions. *Bull Seismol Soc Am* 98(4):1964–1974. doi:10.1785/0120070131
- Rovida A, Camassi R, Gasperini P, Stucchi M (2011) CPTI11, the 2011 version of the parametric catalogue of Italian earthquakes. Milano, Bologna, <http://emidius.mi.ingv.it/CPTI>, doi:10.6092/INGV.IT-CPTI11
- Saccorotti G, Bianco F, Castellano M, Del Pezzo E (2001) The July–August 2000 seismic swarms at Campi Flegrei volcanic complex, Italy. *Geophys. Res. Lett.* 28(13):2525–2528
- Saccorotti G, Petrosino S, Bianco F, Castellano M, Galluzzo D, La Rocca M, Del Pezzo E, Zaccarelli L, Cusano P (2007) Seismicity associated with the 2004–2006 renewed ground uplift at Campi Flegrei Caldera, Italy. *Phys Earth Planet Inter* 165:14–24
- Selva J, Orsi G, Di Vito M, Marzocchi W, Sandri L (2011) Probability hazard map for future vent opening at the Campi Flegrei caldera. *Bull Volcanol, Italy*. doi:10.1007/s00445-011-0528-2
- Snoke AJ (2003) FOCMEC: FOCal MEchanism determination. *Int Geophys*. doi:10.1016/S0074-6142(03)80291-7
- Tramelli A, Galluzzo D, Del Pezzo E, Di Vito MA (2010) A detailed study of the site effects at the volcanic area of Campi Flegrei using empirical approaches. *Geophys J Int* 182(2):1073–1086